STELLAR AGE DETERMINATIONS IN TARGET SELECTION STRATEGY

FOR THE SETI MICROWAVE OBSERVING PROJECT

Final report to the

Space Telescope Science Institute

by

Sallie L. Baliunas
Astrophysicist
Smithsonian Astrophysical Observatory
60 Garden Street
Cambridge MA 02138

(617) 495-7415

AGE DETERMINATION OF CANDIDATE SOLAR-TYPE DWARFS

The ages of candidate stars for the SETI search are critical to ensure that stars of sufficient age – that is, approximately solar age – are selected. We report results of initial observations of and analysis from a 3-year observing program that sought to determine the ages of a subset of stars determined from the larger sample to be single stars close to the sun in spectral type (F9 V to K0 V). The results from are being prepared for publication.

Ages of single, solar-type stars in the field can be efficiently determined from a measurement of the relative strength of the Ca II H and K emission lines. Moreover, the strength of chromospheric emission lines such as the H and K lines is the most precise and unambiguous measurement of main-sequence age. Other determinations of stellar ages, for example, from lithium abundance, *vsini* or kinematics involve difficult measurements, interpretation or analysis, resulting in ambiguity of the determination of age. The H and K emission strengths are straightforward to measure and interpret and can yield a high degree of accuracy in inferred ages (Soderblom et al. 1991, *Ap.J.*, 375, 722) and can yield results for a large sample of stars in a short amount of time.

In the initial phase of the observing program, we constructed the function that best characterizes age as a function of stellar magnetic activity, as indicated by the relative flux in the Ca II H and K emission cores. The observations were from two sources: either stars previously observed at Mount Wilson or independent measurements that could be transformed to the Mount Wilson index of chromospheric activity. This yielded a good, initial function that could be used to determine ages based on measurement of the relative H and K flux. The newly-determined function of lower main sequence age as a function of chromospheric emission flux is different from that of Soderblom et al (1991) for young stars. However, for the purposes of finding old stars, the difference in the two functions is inconsequential.

Next we observed 102 lower main sequence stars (Table 1 and Figure 1) at a sampling frequency of a few measurements per observing season. Young stars (ages less than 1 - 2 gigayr) were easily distinguished from old stars in our extended sample on the basis of the initial, averaged measurement. the histogram of ages in the program stars are shown in Figure 2. Note the apparently extraordinarily old star, at an age of 18.5 Gigayr. The observation is secure; follow-up work is being done to investigate the cause of the result of the great age implied.

The second phase of the program focused on the stars with relatively weak H and K chromospheric emission, i.e., the stars with ages of several billion years or so. Subsequent to the determination of an approximate age in the sample, intensive measurements were made on a schedule of several times per week in a subset of 50 stars from the new sample that proved to be close in mass and age to the sun. These frequent measurements were made in order to assess variability on short time scales due to rotation modulation and the growth and decay of active regions, as well as to determine rotation. Rotation modulation may add as much as 10 to 15 per cent scatter to the instantaneous or undersampled relative flux, and would be a source of uncertainty in determining ages.

Since rotation decreases with increasing main sequence age, the determination of rotation *periods* could serve as an independent check of the age determined from the average chromospheric emission strength. The rotation period may be the most accurate way of determining ages, because, as we have discovered, stars close in mass and age to the sun undergo activity cycle variations on time scales of a decade, and even larger-amplitude variations on time scales of centuries. An example of the latter variations is the Sun during the Maunder Minimum of the 17th century, when activity dropped to very low levels, much lower that at the minimum phase between sunspot cycles. An instantaneous flux measurement would yield an age with large uncertainty, depending on the phase of long-term variations. In addition, direct observation of the rotation period eliminates the ambiguity arising from measurement of the Doppler broadening in spectral lines, because the Doppler broadening indicates the projected rotational velocity, $v sin i$.

Table 1 lists the results of the stellar observing program. Column 1 lists the mean S-value, Col. 2 is the rms of the mean S, Col. 3 is the number of observations, Col. 4 is the number of nights the star was observed, Col. 5 is R'_{HK}, in units of 10^5, Col. 6 is log of the convective turnover time, τ, and Col. 7 is the HD number of the star.

Further analysis revealed the existence of uncertainty in the determination of ages of stars close in mass and age to the sun. As described above, the long-term variability of sun-like stars leads to a substantial uncertainty in age determination when the phase of long-term variability is unknown. In the case of the Sun, five different phases of long-term activity serve to show the uncertainty in the age determination. The fluxes at sunspot minimum, maximum and between them yield ages within one gigayr. The sun spends approximately two-thirds of its time in cyclic state, so this is an accurate range of uncertainty in age determination for two out of three stars if the phase of the sunspot cycle is not known. However, for roughly one-third of the time, the sun's magnetic activity rises to extraordinarily high or low states of magnetic activity, yielding an age that is as young as 3 gigayr or as old as 8 gigayr. Thus, the age determination carries with it an uncertainty that can be characterized by a probability distribution depending on the amount of time the star spends at each phase. That information is best known for the sun, and mostly unknown for individual stars.

Figure 3 shows the chromospheric activity of all the stars in the Mount Wilson data base, including the stars observed for this program. The five states of solar activity are indicated by the large dots connected by the vertical line.

An additional, independent estimate of the uncertainty in age due to long-term phases of chromospheric variation is being made by comparing the ages obtained from components of widely-separated binaries, which are assumed to be coeval. Perfect agreement in the age determination for a binary would be revealed by the same age; many of the pairs of components of binary stars show significantly different ages, indicating long-term variability that is undersampled in our brief measurements of fluxes.

A third way to estimate the uncertainty of the age determination is to observe the instantaneous spread in a substantial sample of coeval stars. We (along with R. Gilliland, Space Telescope Science Institute) observed the early G-type stars in the old, open cluster, M67. We used the 4-meter telescope at Kitt Peak National Observatory, and the Hydra fiber feed and echelle to record the spectra of about 200 stars in M67 with the same spectral coverage as the Mount Wilson instrument. The data are currently being reduced.

Figure Captions

Figure 1 – Average chromospheric magnetic activity as a function of $(B-V)$-color index in the sample of possible SETI target stars observed in this program. For comparison, the Sun is indicated by the large, open circle.

Figure 2 – Histogram of ages of stars in the possible SETI sample from Figure 1. The binsize is 500 million years.

Figure 3 – Average chromospheric magnetic activity vs. mass for the entire sample of stars in the Mount Wilson data base. The sun at five different phases of long-term magnetic activity is denoted by the five dots connected with a vertical line.

Table 1. Results from Possible Candidate SETI Targets

$<S>$	rms	N_{obs}	N_{nights}	$R'_{HK} x 10^5$	$log \tau$	$HD Number$
0.2043	0.0317	201	67	1.5653	9.4376	224930
0.2721	0.0422	117	39	2.4374	9.1445	123
0.1527	0.0237	126	42	0.9365	9.7911	1388
0.1516	0.0234	117	39	0.8269	9.8717	1461
0.3542	0.0601	259	86	3.7074	8.7341	1835
0.2257	0.0933	45	13	1.6348	9.4078	3443
0.1549	0.0243	93	31	0.8345	9.8659	3795
0.1459	0.0226	108	36	0.8237	9.8742	4307
0.1675	0.0259	39	13	1.0177	9.7355	6582
0.1982	0.0307	135	45	1.6523	9.4006	6920
0.1365	0.0211	435	143	0.6625	10.0053	9562
0.1482	0.0231	39	13	0.7665	9.9190	10145
0.1488	0.0228	81	27	0.8625	9.8448	10307
0.1706	0.0261	207	69	0.9822	9.7594	10700
0.1477	0.0229	61	21	0.7115	9.9639	10697
0.1486	0.0229	228	77	0.8596	9.8470	12235
0.1467	0.0227	96	33	0.8302	9.8692	13043
0.4087	0.0632	63	21	4.9709	(7.7761)	16397
0.1406	0.0216	54	18	0.7449	9.9364	19373
0.3358	0.0532	255	85	3.2893	8.8991	20630
0.3829	0.0594	222	74	3.7138	8.7312	26913
0.2853	0.0442	217	73	3.0623	8.9716	26923
0.3068	0.0478	116	40	3.2308	8.9187	30495
0.1680	0.0592	66	22	1.1559	9.6482	30562
0.1516	0.0241	72	24	0.9178	9.8044	33093
0.1443	0.0227	51	17	0.7940	9.8972	34411
0.3306	0.0540	308	103	3.7867	8.6967	39587
0.1505	0.0236	91	31	0.8551	9.8503	39881
0.1449	0.0226	51	18	0.8124	9.8829	41330
0.1531	0.0236	228	77	0.9354	9.7919	43587
0.1509	0.0237	66	22	0.9344	9.7926	48682
0.1571	0.0244	120	40	1.0219	9.7327	50692
0.1586	0.0247	111	37	1.0295	9.7277	52711
0.1532	0.0237	81	27	0.9589	9.7754	55575
0.1647	0.0257	123	41	1.1243	9.6674	64096
0.1672	0.0259	66	22	0.9664	9.7702	65583
0.1728	0.0267	105	35	1.1095	9.6765	68017
0.1683	0.0262	129	43	0.8459	9.8573	69830
0.1360	0.0210	126	42	0.6720	9.9972	70110
0.1549	0.0240	72	24	0.9481	9.7830	71148
0.3595	0.0564	85	28	4.0830	8.5352	72905
0.2345	0.0369	189	63	1.9801	9.2799	76151
0.2514	0.0403	327	109	2.4912	9.1299	78366
0.2421	0.0566	87	31	1.7734	9.3529	79096
0.1736	0.0272	273	90	1.2088	9.6171	81809
0.1363	0.0212	79	27	0.6708	9.9982	84737
0.1445	0.0224	96	32	0.7565	9.9270	86728
0.1657	0.0260	69	25	1.1409	9.6572	88725
0.1555	0.0240	87	29	0.9800	9.7609	90508
0.1463	0.0225	90	31	0.8290	9.8701	95128
0.3285	0.0511	243	81	3.6587	8.7560	97334
0.3134	0.0552	414	137	2.6739	9.0807	101501
0.1853	0.0293	177	59	1.0554	9.7108	103095
0.1590	0.0244	93	31	1.0429	9.7189	109358
0.1582	0.0245	126	44	0.9330	9.7936	114174
0.1899	0.0297	471	156	1.5681	9.4364	114710

0.3264	0.0524	144	48	3.6740	8.7492	115043
0.3312	0.0618	183	60	3.8411	8.6698	115383
0.1621	0.0252	162	54	0.9041	9.8143	115617
0.1414	0.0222	73	24	0.6506	10.0157	117176
0.1371	0.0211	129	43	0.6813	9.9892	120066
0.1713	0.0265	69	23	0.9352	9.7920	122742
0.1479	0.0230	131	46	0.8603	9.8465	124553
0.1687	0.0261	150	50	1.1557	9.6483	126053
0.5779	0.0928	297	100	7.5304	(1.5530)	129333
0.4827	0.0970	552	183	4.0523	8.5537	131156A
0.1606	0.0249	307	104	1.0601	9.7077	141004
0.1711	0.0266	63	21	1.2367	9.6013	142267
0.1495	0.0232	708	229	0.8858	9.8276	143761
0.1686	0.0264	75	25	0.9327	9.7938	144579
0.1806	0.0337	3	1	1.0054	9.7436	145958A
0.1826	0.0345	3	1	1.0259	9.7300	145958B
0.1831	0.0313	147	49	1.3247	9.5533	146233
0.4242	0.0716	512	170	3.4561	8.8390	152391
0.1853	0.0311	63	21	1.1237	9.6677	154345
0.1563	0.0245	159	53	0.9772	9.7628	157214
0.1627	0.0252	165	54	0.8893	9.8250	158614
0.1765	0.0278	150	50	1.2513	9.5931	159222
0.1348	0.0211	249	83	0.6291	10.0345	161239
0.4822	0.0748	120	40	5.8679	(6.4160)	165401
0.1532	0.0240	150	50	0.8950	9.8208	168009
0.1794	0.0279	291	99	1.3702	9.5298	176051
0.1804	0.0285	153	51	1.3988	9.5154	176377
0.1525	0.0239	276	96	0.8042	9.8892	178428
0.1486	0.0230	132	46	0.7713	9.9151	179957
0.1515	0.0235	132	44	0.8697	9.8395	179958
0.1659	0.0269	153	51	1.0184	9.7350	181655
0.1399	0.0221	69	23	0.6186	10.0438	183650
0.1494	0.0231	54	18	0.8524	9.8524	186408
0.1474	0.0228	54	18	0.7972	9.8947	186427
0.1892	0.0299	90	30	1.5413	9.4482	189340
0.1472	0.0232	243	81	0.6873	9.9841	190360
0.1886	0.0294	360	122	1.4863	9.4733	190406
0.1618	0.0249	81	27	1.0981	9.6836	193664
0.1420	0.0223	36	12	0.6862	9.9851	195564
0.1560	0.0245	123	41	0.9800	9.7609	196850
0.1900	0.0441	127	45	1.4507	9.4901	197076
0.1463	0.0228	90	30	0.8194	9.8775	199960
0.1570	0.0653	42	10	0.3840	10.2700	202573
0.3305	0.0511	447	151	3.7857	8.6972	206860
0.1510	0.0236	63	21	0.7116	9.9638	210277
0.1470	0.0226	212	73	0.7784	9.9095	217014

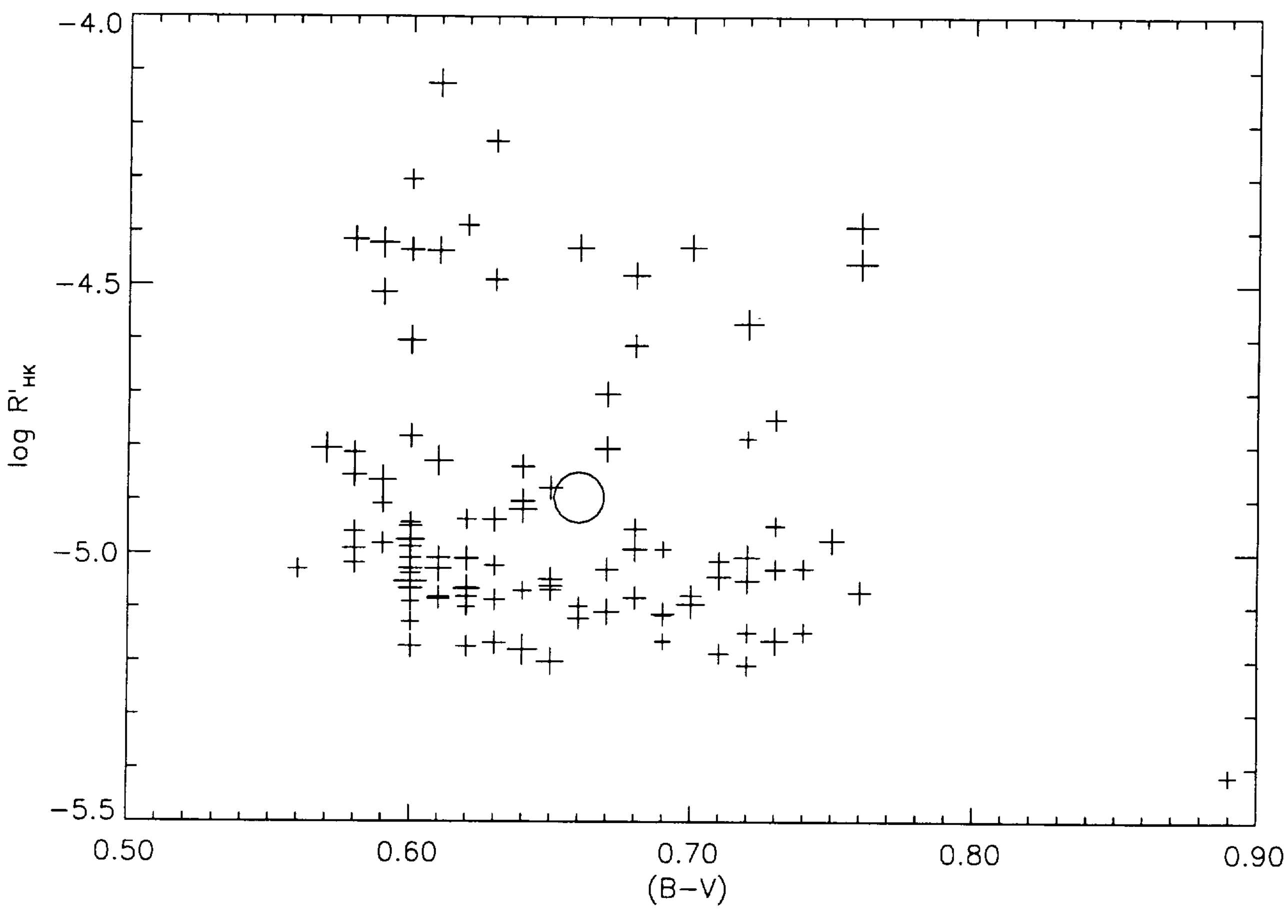

Figure 1

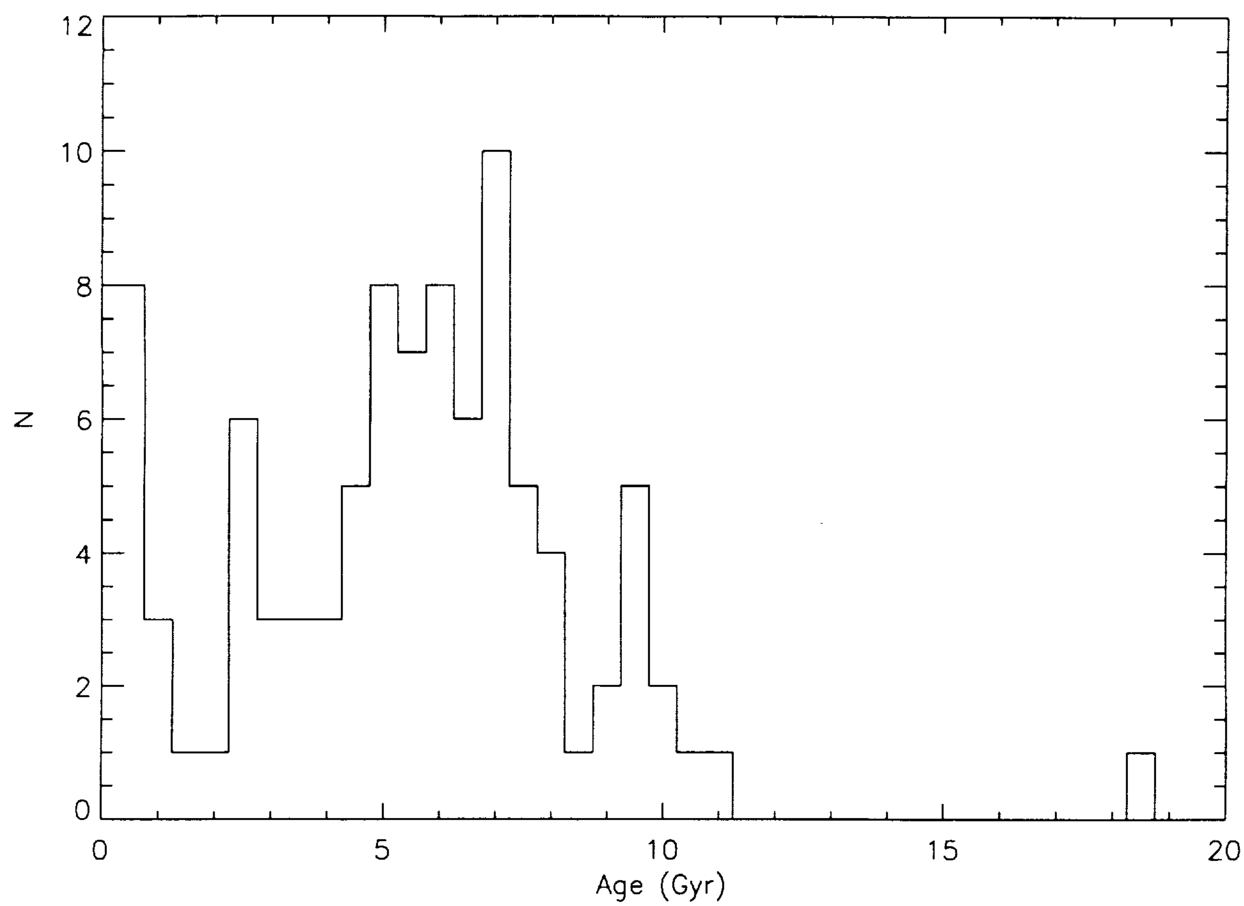

Figure 2

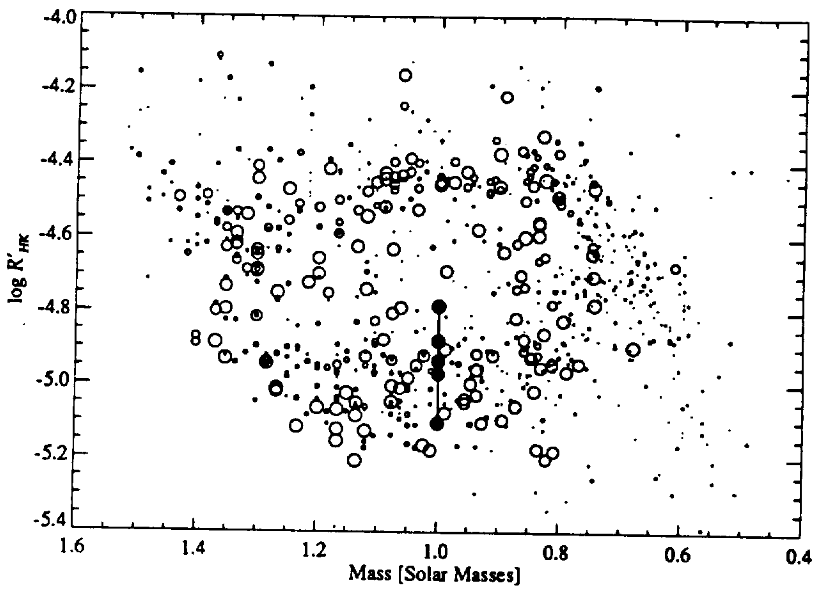

-4.0
-4.2
-4.4
-4.6
-4.8
-5.0
-5.2
-5.4
log R'_{HK}
1.6
1.4
1.2
1.0
0.8
0.6
0.4
Mass [Solar Masses]

Figure 3